Analytical Modelling of HVDC Transmission System Converter using Matlab/Simulink

Rajiv Kumar, Thomas Leibfried

Abstract—. Deeper insight into the functioning of complex HVDC transmission system converter can be obtained by analytical modelling. Further easy to comprehend analytical model in universally available software like Matlab/Simulink can help in fast spread of complex HVDC system knowledge also to those who are responsible for operation and maintenance of these systems thus bringing large benefits. With this in view, a simple analytical model using Matlab/Simulink has been developed in this work to investigate the steady state operation of the 6 pulse single bridge HVDC transmission system converter. The model is based on dividing each cycle of the 60 Hz system into twelve intervals out of which six intervals are commutation intervals with three valves conducting. The system performance for each of the 12 interval has been captured using differential equations applicable for particular interval. These equations have then been converted into integral form followed by Laplace representation to develop the 6 pulse HVDC model in Matlab/Simulink. Steady state operation of the system has been investigated by observing the DC circuit current, commutation process, current and voltage in transformer windings, and source current in time domain. Further the performance of tuned filters for 5^{th}, 7^{th}, 11^{th} and, 13^{th} harmonics and high pass filters has been observed in time domain. Determination of commutation overlap angle by iterative process using the model has been demonstrated. This contribution can be very useful particularly for the operation and maintenance personnel who can perform better with greater insight into the functioning of the complex system obtained through the model as developed.

Index Terms-- HVDC transmission system, converter, tuned filters, high pass filter, thyristor valve, firing angle, overlap angle, time domain simulation.

R. Kumar*, T. Leibfried are with Institute of Electric Energy Systems and High-Voltage Technology (IEH), University of Karlsruhe (TH),
Kaiserstr. 12, 76128 Karlsruhe, Germany (Telephone : +49 / 721 / 608-6125, fax. : +49 / 721 / 69 52 24,
e-mail: kumar@ieh.uni-karlsruhe.de (*))

I. INTRODUCTION

ADVANCEMENTS in power electronics are making High Voltage Direct Current Transmission Systems (HVDC) more and more attractive and reliable. Developing countries like India and China with their ambitious power capacity enhancement program are installing more HVDC systems for long distance transmission. More can be obtained from huge investments in complex HVDC systems if operation and maintenance personnel have deeper understanding about the functioning of these systems. Further commissioning/ maintenance errors may be minimized if the consequences of such errors are known and appreciated by the concerned personnel. Easy to comprehend, simple analytical HVDC converter model as developed in universal software Matlab/Similink in this paper can prove to be very useful for operation and maintenance personnel. The model illustrates steady state operation of HVDC system converter and can be used to comprehend commutation and overlap, valve firing sequence, AC current and voltage waveforms in converter transformer & the source, and DC current including ripple. The model also helps in understanding the role and importance of AC filters. The model has been realized using simple block and switches (without any thyristor block) as available in universal version of Matlab/Simulink.

II. METHODOLOGY

The six pulse converter system including AC filters considered for modelling is shown in Fig. 1. For representing the system by differential equations, each time period of 0.01666s (60Hz system) has been divided into 12 intervals t_1 through t_{12} out which 6 intervals viz t_1, t_3, t_5, t_7, t_9, t_{11} correspond to commutation from one valve to the respective other valve as illustrated in Fig.2 (middle). Gate **Pulse-1** switches on Valve 3 (Th3) when pre-specified delay (corresponding to firing angle - α) occurs after Phase-S voltage crosses Phase-R voltage at point **A** marked in Fig.2 (top). Thus during time interval t_1, three valves viz. Th1, Th2,& Th3 conduct and current flow path is as shown in Fig.1. During this interval commutation takes place and the current i_p in the outgoing Phase-R of the converter transformer

(with an initial magnitude equal to the DC circuit current) reduces to zero as shown in Fig.2 (bottom). Whereas the current in Phase-S of the transformer with an initial magnitude equal to zero increases to magnitude equal to that of the DC circuit current during this interval. In the next time interval t_2, current equal to DC circuit current magnitude flows in phase Phase-S and Phase-T. During this interval no current flows through Phase-R of the converter transformer. Current flow in the remaining time intervals t_3 through t_{12} can also be understood like this.

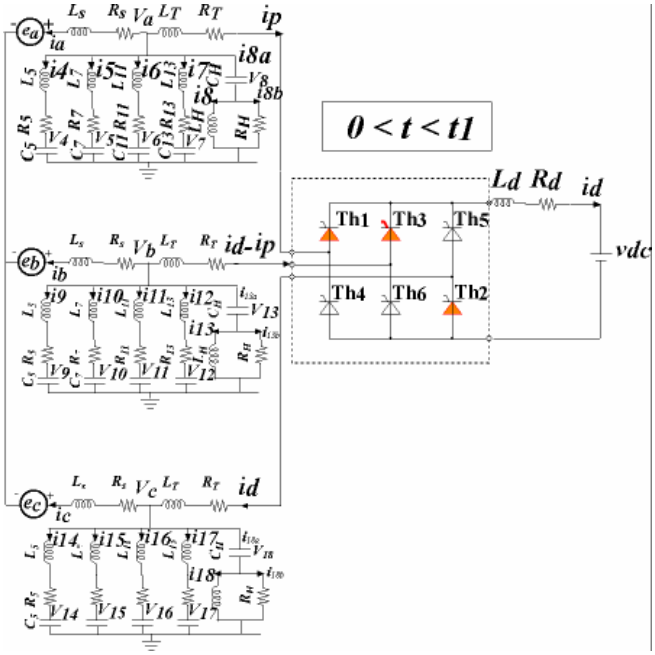

Fig. 1. Schematic of six pulse converter system.

For the purpose of building an analytical model, differential equations of the converter system for each of the time intervals t_1 through t_{12} are developed first in the integral form and then transformed into *s*- space. These equations are further resolved with additional variables to get equations given in *Table 2* and *Table 3*. Nomenclature used is given in *Table 1*. Equations given in Table 2 are common for all the intervals t_1 through t_{12} but those given in Table 3 are different for each of the 12 intervals. The equations for each interval depend on i) whether there is current in all the three phases of the converter transformer (during commutation intervals) or only in two phases when there is no commutation and ii) the direction of current flow in the transformer winding during the interval under consideration. The detailed basis for developing these equations can be found in references [6], [7], and [10]. Based on the equations given in *Table 2* and *Table 3*, we have developed the Matlab/Simulink models for each of the variables. Typical example of the model as developed for direct current current i_d is illustrated in Fig.3. Each of the switching positions of the "Twelve position switch" as shown in Fig.3 corresponds to the time interval t_1 through t_{12}. For example when the switch is in position 1, the computation of i_d is done using equations applicable for time interval t_1.

Table 1 - Nomenclature

Quantity	Symbol	*Quantity*	Symbol
Voltage	V	Current	i
Resistance	R	Inductance	L
Capacitance	C	Time	t
Laplace operatror	s	Source voltage	e

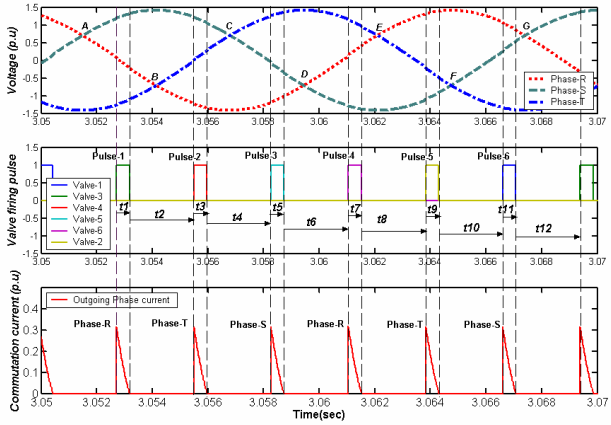

Fig. 2.Illustration of time interval concept: Time function of (1) transformer voltages for phase-R, phase- S and phase- T (2) valve firing pulses and (3)

The length of t_1 depends on commutation overlap on completion of which the "Twelve position switch" switches to position 2, so that i_d is now calculated based on equations corresponding to interval t_2 and so on for the other intervals. Since the integral block used is common for all the intervals, continuity of i_d is ensured from interval to the next interval.

Table 2 – Equations common for all intervals t_1 through t_{12}.

Circuit	*Voltage*	*Current*
Phase-R	$V_4 = \frac{1}{C_5.s} i_4$ $V_5 = \frac{1}{C_7.s} i_5$ $V_6 = \frac{1}{C_{11}.s} i_6$ $V_7 = \frac{1}{C_{13}.s} i_7$ $V_8 = \frac{-1}{C_H.s}\{i_{t_R}\}$ $V_a = V_8 - R_H(i_{t_R} + i_8)$	$i_4 = \frac{1}{L_5.s}\{V_a - V_4 - R_5 i_4\}$ $i_5 = \frac{1}{L_7.s}\{V_a - V_5 - R_7 i_5\}$ $i_6 = \frac{1}{L_{11}.s}\{V_a - V_6 - R_{11} i_6\}$ $i_7 = \frac{1}{L_{13}.s}\{V_a - V_7 - R_{13} i_7\}$ $i_8 = \frac{-R_H}{L_H.s}\{i_{t_R} + i_8\}$ $i_a = \frac{1}{L_s.s}\{V_a - e_a - R_s i_a\}$
Phase-S	$V_9 = \frac{1}{C_5.s} i_9$ $V_{10} = \frac{1}{C_7.s} i_{10}$ $V_{11} = \frac{1}{C_{11}.s} i_{11}$ $V_{12} = \frac{1}{C_{13}.s} i_{12}$ $V_{13} = \frac{-1}{C_H.s}\{i_{t_S}\}$ $V_b = V_{13} - R_H(i_{t_S} + i_{13})$	$i_9 = \frac{1}{L_5.s}\{V_b - V_9 - R_5 i_9\}$ $i_{10} = \frac{1}{L_7.s}\{V_b - V_{10} - R_7 i_{10}\}$ $i_{11} = \frac{1}{L_{11}.s}\{V_b - V_{11} - R_{11} i_{11}\}$ $i_{12} = \frac{1}{L_{13}.s}\{V_b - V_{12} - R_{13} i_{12}\}$ $i_{13} = \frac{-R_H}{L_H.s}\{i_{t_S} + i_{13}\}$ $i_b = \frac{1}{L_s.s}\{V_b - e_b - R_s i_b\}$
Phase-T	$V_{14} = \frac{1}{C_5.s} i_{14}$ $V_{15} = \frac{1}{C_7.s} i_{15}$ $V_{16} = \frac{1}{C_{11}.s} i_{16}$ $V_{17} = \frac{1}{C_{13}.s} i_{17}$ $V_{18} = \frac{-1}{C_H.s}\{i_{t_T}\}$ $V_c = V_{18} - R_H(i_{t_T} + i_{18})$	$i_{14} = \frac{1}{L_5.s}\{V_c - V_{14} - R_5 i_{14}\}$ $i_{15} = \frac{1}{L_7.s}\{V_c - V_{15} - R_7 i_{15}\}$ $i_{16} = \frac{1}{L_{11}.s}\{V_c - V_{16} - R_{11} i_{16}\}$ $i_{17} = \frac{1}{L_{13}.s}\{V_c - V_{17} - R_{13} i_{17}\}$ $i_{18} = \frac{-R_H}{L_H.s}\{i_{t_T} + i_{18}\}$ $i_c = \frac{1}{L_s.s}\{V_c - e_c - R_s i_c\}$

However for commutation current i_p, separate and dedicated integral block has been used for each of the six commutating intervals t_1, t_3 t_5, t_7, t_9 and t_{11}. Further each of these integral blocks i) is reset by the switching pulse at the beginning of

respective interval, and ii) picks up the corresponding instantaneous value of i_d as initial value. This ensures that the current i_p in the outgoing phase commutates from initial value i_d to final value equal to 0.

Table 3 - Equations different for each intervals t_1 through t_{12}.

Interval/ Variable value	*Interval/ Variable value*
t_1 $i_{t_R} = \{i_4 + i_5 + i_6 + i_7 + i_a + i_p\}$ $i_{t_S} = \{i_9 + i_{10} + i_{11} + i_{12} + i_b + i_d - i_p\}$ $i_{t_T} = \{i_{14} + i_{15} + i_{16} + i_{17} - i_d + i_c\}$	t_1 $i_d = \frac{1}{(3L_T+2L_d).s}\{-3V_c - 2V_{dc} - (3R_T + 2R_d)i_d\}$ $i_p = \frac{-1}{L_T.s}\{-V_b - V_c + \frac{(R_dL_T - L_dR_T)}{(3L_T+2L_d)}i_d + i_pR_T + \frac{L_T}{(3L_T+2L_d)}V_{dc}\}$
t_2 $i_{t_R} = \{i_4 + i_5 + i_6 + i_7 + i_a\}$ $i_{t_S} = \{i_9 + i_{10} + i_{11} + i_{12} + i_b + i_d\}$ $i_{t_T} = \{i_{14} + i_{15} + i_{16} + i_{17} - i_d + i_c\}$	t_2 $i_d = \frac{1}{(2L_T+L_d).s}\{V_b - V_c - V_{dc} - (2R_T + R_d)i_d\}$
t_3 $i_{t_R} = \{i_4 + i_5 + i_6 + i_7 + i_a - (i_d - i_p)\}$ $i_{t_S} = \{i_9 + i_{10} + i_{11} + i_{12} + i_b + i_d\}$ $i_{t_T} = \{i_{14} + i_{15} + i_{16} + i_{17} - i_p + i_c\}$	t_3 $i_d = \frac{1}{(3L_T+2L_d).s}\{3V_b - 2V_{dc} - (3R_T + 2R_d)i_d\}$ $i_p = \frac{-1}{L_T.s}[V_a + V_b + \frac{(R_dL_T - L_dR_T)}{(3L_T+2L_d)}i_d + i_pR_T + \frac{L_T}{(3L_T+2L_d)}V_{dc}]$
t_4 $i_{t_R} = \{i_4 + i_5 + i_6 + i_7 + i_a - i_d\}$ $i_{t_S} = \{i_9 + i_{10} + i_{11} + i_{12} + i_b + i_d\}$ $i_{t_T} = \{i_{14} + i_{15} + i_{16} + i_{17} + i_c\}$	t_4 $i_d = \frac{1}{(2L_T+L_d).s}\{V_b - V_a - V_{dc} - (2R_T + R_d)i_d\}$
t_5 $i_{t_R} = \{i_4 + i_5 + i_6 + i_7 + i_a - i_d\}$ $i_{t_S} = \{i_9 + i_{10} + i_{11} + i_{12} + i_b + i_p\}$ $i_{t_T} = \{i_{14} + i_{15} + i_{16} + i_{17} + i_d - i_p - i_c\}$	t_5 $i_d = \frac{1}{(3L_T+2L_d).s}\{-3V_a - 2V_{dc} - (3R_T + 2R_d)i_d\}$ $i_p = \frac{-1}{L_T.s}[-V_c - V_a + \frac{(R_dL_T - L_dR_T)}{(3L_T+2L_d)}i_d + i_pR_T + \frac{L_T}{(3L_T+2L_d)}V_{dc}]$
t_6 $i_{t_R} = \{i_4 + i_5 + i_6 + i_7 + i_a - i_d\}$ $i_{t_S} = \{i_9 + i_{10} + i_{11} + i_{12} + i_b\}$ $i_{t_T} = \{i_{14} + i_{15} + i_{16} + i_{17} + i_c + i_d\}$	t_6 $i_d = \frac{1}{(2L_T+L_d).s}\{V_c - V_a - V_{dc} - (2R_T + R_d)i_d\}$
t_7 $i_{t_R} = \{i_4 + i_5 + i_6 + i_7 + i_a - i_p\}$ $i_{t_S} = \{i_9 + i_{10} + i_{11} + i_{12} + i_b - (i_d - i_p)\}$ $i_{t_T} = \{i_{14} + i_{15} + i_{16} + i_{17} + i_d + i_c\}$	t_7 $i_d = \frac{1}{(3L_T+2L_d).s}\{3V_c - 2V_{dc} - (3R_T + 2R_d)i_d\}$ $i_p = \frac{-1}{L_T.s}[V_b + V_c - \frac{(R_dL_T + L_dR_T)}{(3L_T+2L_d)}i_d + i_pR_T + \frac{L_T}{(3L_T+2L_d)}V_{dc}]$
t_8 $i_{t_R} = \{i_4 + i_5 + i_6 + i_7 + i_a\}$ $i_{t_S} = \{i_9 + i_{10} + i_{11} + i_{12} + i_b - i_d\}$ $i_{t_T} = \{i_{14} + i_{15} + i_{16} + i_{17} + i_c + i_d\}$	t_8 $i_d = \frac{1}{(2L_T+L_d).s}\{V_c - V_b - V_{dc} - (2R_T + R_d)i_d\}$
t_9 $i_{t_R} = \{i_4 + i_5 + i_6 + i_7 + i_a + i_d - i_p\}$ $i_{t_S} = \{i_9 + i_{10} + i_{11} + i_{12} + i_b - i_d\}$ $i_{t_T} = \{i_{14} + i_{15} + i_{16} + i_{17} + i_p + i_c\}$	t_9 $i_d = \frac{1}{(3L_T+2L_d).s}\{-3V_b - 2V_{dc} - (3R_T + 2R_d)i_d\}$ $i_p = \frac{-1}{L_T.s}[-V_a - V_b + \frac{(R_dL_T - L_dR_T)}{(3L_T+2L_d)}i_d + i_pR_T + \frac{L_T}{(3L_T+2L_d)}V_{dc}]$
t_{10} $i_{t_R} = \{i_4 + i_5 + i_6 + i_7 + i_a + i_d\}$ $i_{t_S} = \{i_9 + i_{10} + i_{11} + i_{12} + i_b - i_d\}$ $i_{t_T} = \{i_{14} + i_{15} + i_{16} + i_{17} + i_c\}$	t_{10} $i_d = \frac{1}{(2L_T+L_d).s}\{V_a - V_b - V_{dc} - (2R_T + R_d)i_d\}$
t_{11} $i_{t_R} = \{i_4 + i_5 + i_6 + i_7 + i_a + i_d\}$ $i_{t_S} = \{i_9 + i_{10} + i_{11} + i_{12} + i_b - i_p\}$ $i_{t_T} = \{i_{14} + i_{15} + i_{16} + i_{17} - (i_d - i_p) - i_c\}$	t_{11} $i_d = \frac{1}{(3L_T+2L_d).s}\{3V_a - 2V_{dc} - (3R_T + 2R_d)i_d\}$ $i_p = \frac{-1}{L_T.s}[V_c + V_a + \frac{(R_dL_T - L_dR_T)}{(3L_T+2L_d)}i_d + i_pR_T + \frac{L_T}{(3L_T+2L_d)}V_{dc}]$
t_{12} $i_{t_R} = \{i_4 + i_5 + i_6 + i_7 + i_a + i_d\}$ $i_{t_S} = \{i_9 + i_{10} + i_{11} + i_{12} + i_b\}$ $i_{t_T} = \{i_{14} + i_{15} + i_{16} + i_{17} + i_c - i_d\}$	t_{12} $i_d = \frac{1}{(2L_T+L_d).s}\{V_a - V_c - V_{dc} - (2R_T + R_d)i_d\}$

It is important to highlight that the computing equations for all variables i_d, i_p, i_{tR}, i_{tS}, and i_{tT} as indicated in *Table 3* have to be switched simultaneously. Also the switching corresponds to specified time delay (firing angle) after the crossover of the commutation voltages. Moreover no overlap between intervals is permitted. In our model, we have used the "Synchronized six pulse generator" available as standard in Simulink for the commutation intervals. S-R flip flop with triggering on falling and rising pulse of the previous commutation block and the following commutation block respectively have been used for the non commutation intervals. The system data and the a.c. filter parameters used by us for the purpose of model validation are same as given in reference [10].

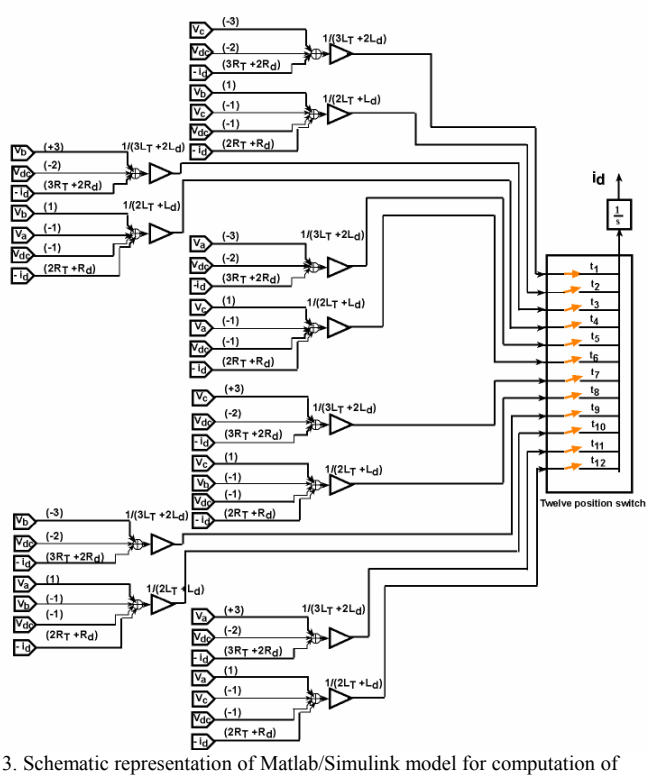

Fig. 3. Schematic representation of Matlab/Simulink model for computation of direct current i_d.

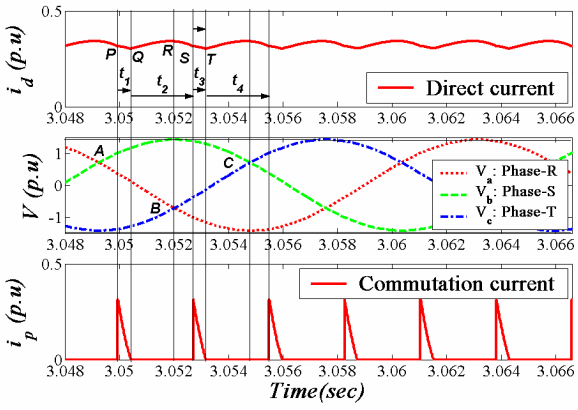

Fig. 4. Time function of (1) direct current i_d (2) transformer voltages V_a, V_b, & V_c for Phase-R, Phase-S, and Phase-T respectively and (3) commutation current i_p.

III. CASE STUDIES

A Steady State Operation of HVDC Transmission System Rectifier

Steady state operation of HVDC transmission system rectifier has been simulated for 15° firing angle. Time function of (1) direct current $\mathbf{i_d}$ (2) transformer voltages $\mathbf{V_a}$, $\mathbf{V_b}$, & $\mathbf{V_c}$ for phase-R, phase-S, and phase-T, respectively and (3)

commutation current $\mathbf{i_p}$ are shown in Fig.4. Root cause of ripple in direct current $\mathbf{i_d}$ can be clearly observed in Fig.4.
Referring to top of Fig.4, at time point **P** commutation of current from phase-R to phase-S begins and is completed at time point **Q.** This is interval $\mathbf{t_1}$ of our model and during this interval $\mathbf{i_d}$ decreases due to decreasing magnitude of $\mathbf{V_c}$ as seen in middle of Fig.4. From time point **Q** to time point **S** the current flows through phase-S and phase-T and there is no current flow in phase-R of the transformer. This is interval $\mathbf{t_2}$ of our model and in this interval $\mathbf{i_d}$ varies in accordance with $(\mathbf{V_b} - \mathbf{V_c})$. It can be seen that within time interval $\mathbf{t_2}$, from time point **Q** to time point **R,** $\mathbf{i_d}$ increases as $\mathbf{V_b}$ is increasing. But from time point **R** to time point **S,** $\mathbf{i_d}$ decreases as $\mathbf{V_b}$ starts falling down after reaching the peak value at point **R.** The decreasing trend of point $\mathbf{i_d}$ continues till time point **T** and when commutation from phase-T to phase-R (negative part of the cycle) is complete, $\mathbf{i_d}$ starts increasing again due to fast increasing magnitude of incoming phase-R. Similar is the case for other intervals.

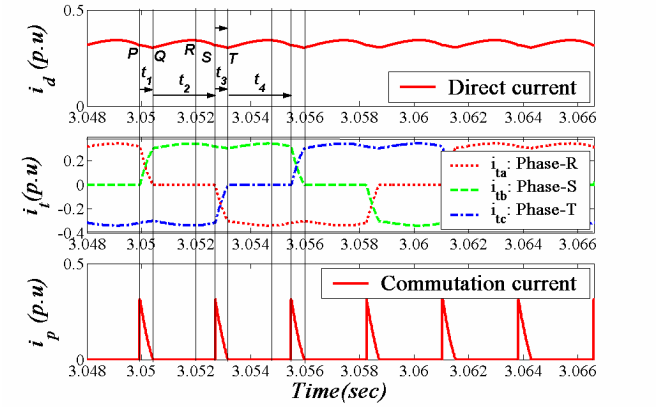

Fig. 5. Time function of (1) direct current $\boldsymbol{i_d}$ (2) transformer currents $\boldsymbol{i_{ta}, i_{tb},}$ & $\boldsymbol{i_{tc}}$ for Phase-R, Phase-S, and Phase-T respectively and (3) commutation current $\boldsymbol{i_p}$.

Time function of (1) direct current $\mathbf{i_d}$ (2) transformer currents $\mathbf{i_{ta}, i_{tb},}$ & $\mathbf{i_{tc},}$ for phase-R, phase-S, and phase-T, respectively and (3) commutation current are shown in Fig.5. Referring to middle of Fig.5, it can be observed that phase-R current starts reducing from a value equal to $\mathbf{i_d}$ at time point **P** to zero at time point **Q** i.e during time interval $\mathbf{t_1}$. At time point **Q** i.e. at the end of time interval $\mathbf{t_1}$, phase-S takes over the entire current $\mathbf{i_d}$ which marks the completion of commutation. Current in phase-R remains zero till time point **S** when it starts taking over from phase-T in the negative cycle. Important to note is that even though the same current as $\mathbf{i_d}$ flows in phase-R from time point **T** onwards (interval $\mathbf{t_4}$) but its direction is reversed as compared to that at the beginning of interval $\mathbf{t_1}$. Also the dents in the transformer phase current wave form can be observed when there is commutation between the other two phases.

Time function of (1) valve currents $\mathbf{i_{Th1}, i_{Th3},}$ & $\mathbf{i_{Th5}}$ (2) valve currents $\mathbf{i_{Th2}, i_{Th4},}$ & $\mathbf{i_{Th6}}$ and (3) commutation current are shown in Fig.6. Commutation of current from valve 1 to 3 during interval $\mathbf{t_1}$ in the positive cycle and from valve 6 to 2 during interval $\mathbf{t_3}$ in the negative cycle and so on for the other valves can be clearly observed.

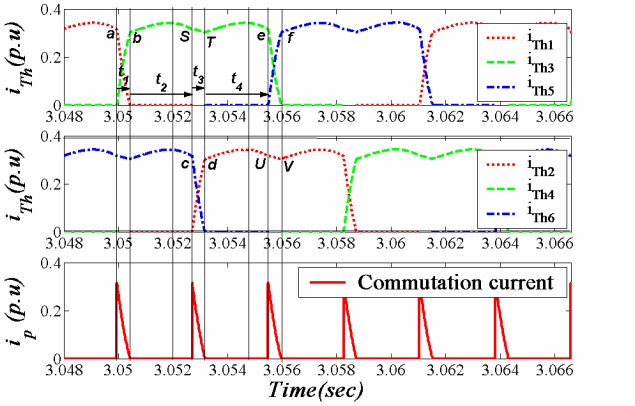

Fig. 6. Time function of (1) valve current $\mathbf{i_{Th1}, i_{Th3},}$ & $\mathbf{i_{Th5}}$ (2) valve current $\mathbf{i_{Th2}, i_{Th4},}$ & $\mathbf{i_{Th6}}$ and (3) commutation current $\boldsymbol{i_p}$.

Time function of (1) transformer currents $\mathbf{i_{ta}, i_{tb},}$ & $\mathbf{i_{tc},}$ for phase-R, phase-S, and phase-T, respectively (2) currents in tuned filter circuits for 5th, 7th, 11th, 13th harmonics and high pass filter and (3) alternating source currents $\mathbf{i_a, i_b,}$ & $\mathbf{i_c,}$ for phase-R, phase-S, and phase-T, respectively are shown in Fig.7. We can clearly observe as to how filters remove the harmonics from trapezoidal shaped current waveform in the transformer windings to give a nearly sinusoidal current waveform in the a.c. source. This figure illustrates the importance of filters from point of view of the source as without the filters source shall be subjected to unwanted harmonic currents.

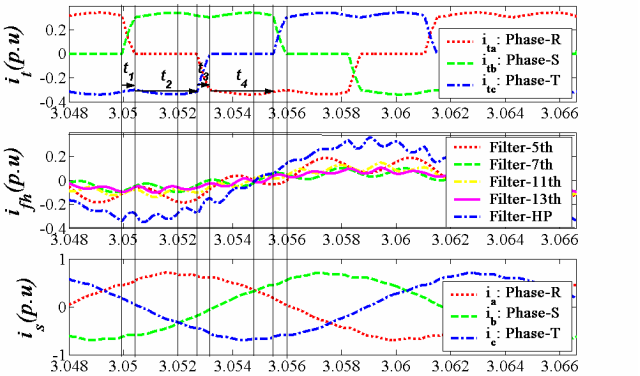

Fig. 7. Time function of (1) transformer currents $\boldsymbol{i_{ta}, i_{tb},}$ & $\boldsymbol{i_{tc}}$ for Phase-R, Phase-S, and Phase-T respectively and (2) current in tuned filters circuits for 5th, 7th, 11th, 13th harmonics and high pass filter and (3) alternating source currents $\boldsymbol{i_{a,}\ i_{tb,}}$ & $\boldsymbol{i_c}$ for Phase-R, Phase-S, and Phase-T respectively.

B Iterative Determination of Overlap Angle

Iterative method can be used to determine the overlap angle and the direct current corresponding to different values of rectifier firing angles using our steady state model. Desired firing angle is set as input to the synchronized six pulse generator and the model is run for different values of overlap

angles. Corresponding commutation current is observed. The

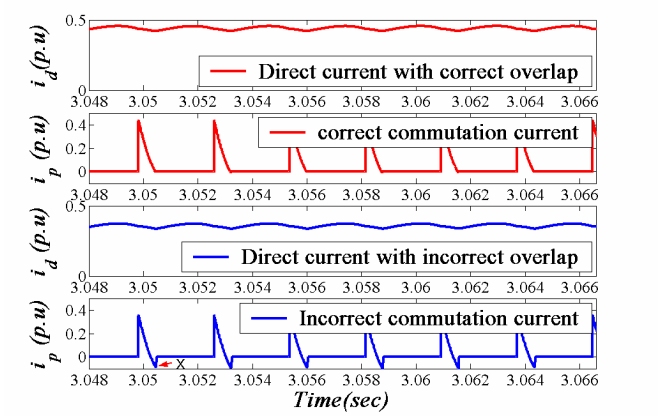

Fig. 8. Time function of (1) direct current i_d with correct ovelap (3) commutation current i_p with correct overlap (3) direct current i_d with incorrect overlap (3) commutation current i_p with incorrect overlap.

commutation current at the end of commutation interval is higher or lower than zero if the overlap angle is lower or higher respectively than the correct value. Thus the correct value of overlap angle is determined as the one which gives zero commutation current at the end of each commutation interval in steady state. This has been illustrated in Fig.8 wherein time function of (1) direct current $\mathbf{i_d}$ with ***correct*** overlap (2) commutation current $\mathbf{i_p}$ for ***correct*** overlap (3) direct current $\mathbf{i_d}$ with *incorrect* overlap and (4) commutation current $\mathbf{i_p}$ for *incorrect* overlap have been plotted. In the lower most part of Fig.8, it can be observed that the commutation current goes below zero value at point ***X*** i.e. at the end of commutation interval. This is an example of a case when overlap angle is more than the correct value. It can also be observed that as expected the direct current for this incorrect overlap angle is much lower than the true value corresponding to the correct overlap as shown in the upper part of Fig.8.

Correct overlap angle can be measured as illustrated in Fig.9. The measured values of overlap angle μ1 for firing angle α = 15˚ is 10.187˚ corresponding to the direct current of 0.34 p.u. Similarly the measured values of overlap angles μ2 for firing angle α = 12.5˚ is 13.157˚ corresponding to the direct current of 0.44 p.u. The corresponding theoretically calculated values of overlap angles are 9.899˚ and 13.32˚ respectively. Thus the measured model result overlap angle values are within 3% of the theoretically calculated values hence compare reasonably well. Thus using the iterative method the model can be utilised to plot the firing angle versus direct current characteristics and determining the corresponding overlap angle.

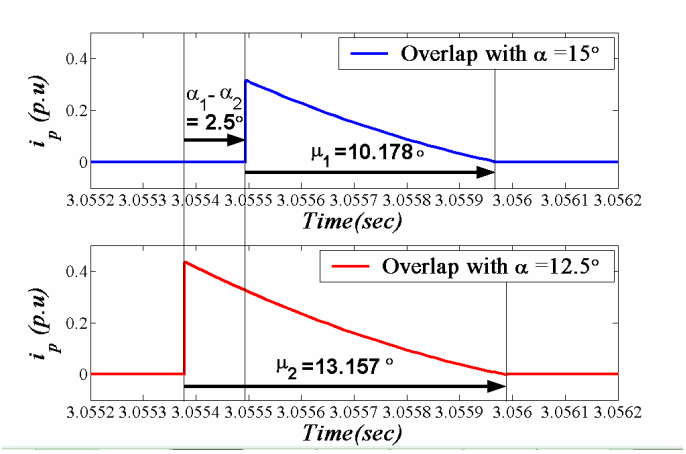

Fig. 9. Measurement of overlap angle (1) overlap with firing angle α = 15˚ and (2) overlap with firing angle α = 12.5˚

IV. CONCLUSION

This paper has clearly demonstrated the methodology for modelling steady state operation of HVDC transmission system rectifier using universally available software Matlab/Simulink. Simulations have been done for different values of firing angle and typical results for 15˚ and 12.5˚ have been reported. The model results are very useful in getting deeper understanding of (1) root cause for ripple in rectifier direct current (2) basis for trapezoidal wave form of rectifier transformer winding current including the dents when other two phases are commutating (3) valve currents in different intervals of each time period and the (4) importance of tuned and high pass filters in extracting the unwanted harmonics from trapezoidal transformer winding current to give nearly sinusoidal source current. Further the model as developed is very useful in plotting the converter system firing angle verses direct current characteristics and determining the corresponding overlap angle in an easy and iterative manner. This contribution can be very useful for HVDC system operation and maintenance personnel who can investigate different operating conditions of HVDC converter system using the model to optimize the system performance. Since Matlab/Simulink as used by us for developing the model are universally available, the HVDC system owners need not invest much in procuring the specialized and costly software for this purpose.

V. REFERENCES

Periodicals:

[1] M.Szechtman, T. Wess, C.V. Thio, " *First benchmark model forHVDC control studies*," ELECTRA, April 1991, pp. 55-73.

[2] M.Szechtman, T. Margaard, J.P. Wowles, C.V. Thio,D.Woodford, T. Wess, R. Joetten, G. Liss, M, Rashwan, P.C. Krishnayya, P.Pavlinec, V. Kovalev, K. Maier,J. gleadow, J.L: Haddock, N.Kaul, R.Bunch, R.Johnson, G.Dellepiane, N. Vovos. " *The CIGRE BenchMark Model – A New Proposal with Revised Parameters*," ELECTRA, December 1994, pp. 61-66.

Books:

[3] HVDC and FACTS Controllers, Vijay. K. Sood, USA, Kluwer Academic Publishers, 2004.

[4] Computer Modelling of Electrical Power Systems, Second Edition, J. Arrillaga, N.R. Watson, Institution of Electrical Engineers, John Wiley & Sons, England, 2001.

[5] Flexible ac transmission systems (FACTS), Jong Hua Song, Allan T. Johns, Institution of Electrical Engineers, London, U.K, 1999.

[6] High Voltage Direct Current Transmission,2nd Edition, Jos. Arrillaga, Institution of Electrical Engineers, London, U.K, 1998.

[7] Direct Current Transmission, Volume I, Edward Wilson Kimbark, Wiley-Interscience, John Wiley & Sons, Canada, 1971.

[8] Power System Stability and Control. New York, Prabha Kundur, McGraw-Hill, Inc., 1993.

[9] Power Transmission by Direct Current, Erich Uhlmann, Springer-Verlag Berlin Heidelberg New York , 1975.

[10] HVDC Power System Transmission Systems, K. R. Padiyar, New Age International(P) Limited, Publishers, !990.

[11] Understanding FACTS, Narain G. Hingorani, Laszlo Gyugyi, IEEE Press, 2000.

[12] Electric Power Transmission System Engineering: Analysis and Design, Turan Gönen, Wiley-Interscience, John Wiley & Sons, USA, 1988.

[13] High Voltage Direct Current Power Transmission, Colin Adamson, N.G. Hingorani, Garraway Limited, London, England, 1960.

[14] Dynamic Modelling of Line and Capacitor Commutated Converters for HVDC Power Transmission, Dissertation Thesis, Wolfgang Hammer, Swiss Fedral Institute of Technology Zurich,Switzerland, 2003.

[15] Analysis of Subsynchronous Resonance in Power Systems, K. R. Padiyar, USA, Kluwer Academic Publishers, 1999.

[16] Multi-Level Inverters for utility-Applications, Olaf Pollakowski, VDI Verlag GmbH, Düsseldorf, Germany, 1999.

VI. BIOGRAPHIES

Rajiv Kumar was born in Junpat, India, in 1958. He received his B.Sc. (Electrical & Electronics) Engineering & Master of Business Administration (MBA), from the University of Delhi, India in 1979 and 1996 respectively and M.Sc. (Electrical Engineering) in 2003 from the Institute of Electric Energy Systems and High-Voltage Technology, University of Karlsruhe, Germany. From 1979 onwards he has been working in National Thermal Power Corporation (NTPC) of India in the engineering department for 17 years (on basic and detailed engineering of new projects, renovation & modernisation of old projects, consultancy projects), erection and commissioning of 432 MW combined cycle Faridabad Gas Power Station for two and a half years, Operation & Maintenance of National Capital Power Station - Dadri (840 MW Coal Fired and 817 MW Combined Cycle Power Plant) for two years as Deputy General Manager. Since December 2001 he is a researcher with the Institute of Electric Energy Systems and High –Voltage Technology, University of Karlsruhe, Germany working in the area of Electric Power System.

Thomas Leibfried was born in Neckarsulm, Germany, in 1964. He studied Electrical Engineering at the University of Stuttgart and received his Dipl.-Ing. and Dr.-Ing. Degree from the University of Stuttgart, Germany, in 1990 and 1996 respectively. He joined Siemens in 1996. After working in the field of transformer monitoring and basics in transformer design Dr. Leibfried changed in 1999 to the quality department as head of the test departments of the transformer factories Nuremberg and Dresden. Beginning from 2001 he worked as Technical Manager in the Service department, where he was responsible for the development of service activities world wide. At the end of 2002 Dr. Lebfried became head of the Institute of Electric Energy Systems, and Professor in the faculty of Electrical and Information Engineering in the University of Karlsruhe, Germany. Prof. Leibfried is member of IEEE and VDE.